MHCNLS-HAR: Multiheaded CNN-LSTM-Based Human Activity Recognition Leveraging a Novel Wearable Edge Device for Elderly Health Care

Neha Gaud, *Member, IEEE*, Maya Rathore, *Member, IEEE*, and Ugrasen Suman, *Senior Member, IEEE*

***Abstract*—Human activity recognition (HAR) systems include the activities performed by a person during daily routines, such as running, walking, and jogging, performed with the help of the lower extremities. This article proposes an HAR system designed for health monitoring, focusing on five gesture categories: walking, running, jumping, squatting, and other activities for data collection. Data collection was carried out using an Arduino Nano 33 Bluetooth Low Energy (BLE) Sense microcontroller, equipped with a 9° inertial measurement unit (IMU) sensor system, at a sampling frequency of 110 Hz. For each gesture, 50 samples are collected from 30 subjects of various age groups (15–65) from the Indian subcontinent (Asian region). All gestures were manifested using the movement of the hip, knee, and ankle joints, which captures the spatial and temporal data of the person during various gestures. This research leverages the power of edge computing devices by fusing the deep learning code over the Arduino Nano microcontroller for gesture recognition. The multiheaded convolutional neural network (CNN) and long short-term memory (LSTM) (MHCNLS)-based deep learning model is proposed to classify the gestures. This model utilizes CNN for spatial dependencies and LSTM for sequential, time series dependencies in the human activity data. The proposed MHCNLS model is evaluated on three benchmark datasets—WISDM, PAMPM2, and UCI-HAR—and our own HEAHL-HAR dataset. The results of the MHCNLS model are compared with various other hybrid deep learning models based on CNN, LSTM, and GRU and their combination to classify the gestures and check the stability of the model. The results are evaluated based on various performance index accuracy, precision, F1-score, recall, and sensitivity. The proposed MHCNLS model has outperformed all existing state-of-the-art models mentioned in the literature with an accuracy of 98.17%. To enable real-time functionality, the MHCNLS model was compressed using pruning and quantization and successfully deployed on an edge computing device with constrained power, data rate, and bandwidth. The model size was reduced by up to five times while maintaining performance accuracy comparable to the uncompressed version. This innovative approach has significant implications for healthcare, rehabilitation, sports, prosthetics, and augmented learning.**

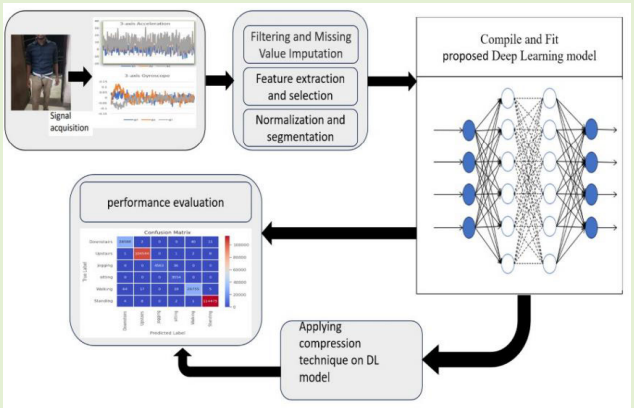

***Index Terms*— Bluetooth Low Energy (BLE) sense, deep learning, edge device, human activity recognition (HAR), tinyML.**

I. Introduction

HUMAN activity recognition (HAR) refers to gestures performed by a human being to execute day-to-day activities [1], [2]. It involves various physiological parameters, neuromuscular interaction, and motor action of muscles [3], [4]. The advent of miniature-based computing and wide sensing technology has paved the way for developing wearable devices to cover various applications domains, including healthcare, gesture recognition, rehabilitation, sports, and fall detection [5], [6]. HAR manifests the gestures performed by the lower extremity, which enables researchers and doctors to track the health of elderly people, diagnosis of various cognitive and pulmonary diseases, degradation of muscle strength, personal fitness, and various health abnormalities at early stages [7], [8].

The detection of HAR can be done by various modalities, which include computer vision and wearable sensor-based techniques. Fig. 1 shows the basic structure of HAR. The widely used sensors are kinetic, inertial measurement sensors,

Manuscript received 29 July 2024; accepted 19 August 2024. Date of publication 5 September 2024; date of current version 31 October 2024. The associate editor coordinating the review of this article and approving it for publication was Prof. Xiaofeng Yuan. *(Corresponding author: Neha Gaud.)*

Neha Gaud and Ugrasen Suman are with the School of Computer Science and Information Technology (SCSIT), DAVV, Indore 30332, India (e-mail: neha28gaud@gmail.com; ugrasen123@yahoo.com).

Maya Rathore is with the Chameli Devi Group of Institutions, Indore 452020, India (e-mail: mayarathore114@gmail.com).

Digital Object Identifier 10.1109/JSEN.2024.3450499

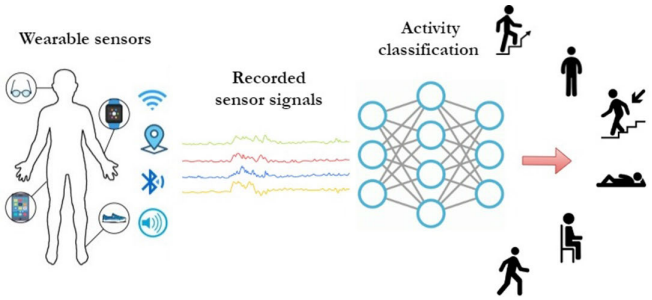

Fig. 1. Basic structure of HAR.

LiDAR sensors, RGB cameras, micro-Doppler radar, and smartphones for HAR recognition system [9]. However, due to issues of backdrop, illumination camera size, and high price, computer vision techniques become expensive, which allows the development of wearable sensor-based HAR systems. These sensors record the signal of various gestures easily. Modern IMU-based systems record the spatial and temporal signals. The HAR signals are made up of spatial and temporal time series data [10]. The other constraint with modern edge devices is low memory size, which cannot run deep learning models. With the help of tinyML, the model size can be compressed and made suitable to this HAR-trained model over small computational edge devices [11].

In this research, a multiheaded convolutional neural network (CNN) long short-term memory (LSTM)-based deep learning model is developed to recognize the five gestures run, walk, jump, squad, and other activities using an IMU sensor embedded with Arduino Nano 33 Bluetooth Low Energy (BLE) sense board. The motions are captured using an accelerometer, magnetometer, and gyroscope, which converts motion into recognizable signals. In conventional models where computational resources are limited, a multiheaded model can provide an efficient way to address the need for multiple tasks without designing multiple models for each task. The model was further compressed to fuse the model on a small-sized Arduino board to leverage the benefits of an Internet-of-Things (IoT)-based edge device. The model is compared with other public datasets also.

The novelty of this work is to identify the gestures in real time using an edge device. It will automate the process of identification of various gestures. Using edge devices will preserve the privacy of data. The size of the model is also a major concern to use in real-time applications. With the advent of the deep learning model, tinyML helps in reducing the size, so it can process over real-time devices. The contribution of this work is listed as follows.

A. Authors' Contribution

The main contribution of this work is the development of a hybrid deep learning model using multiheaded CNN-LSTM (MHCNLS). The different gestures, namely, run, walk, jump, squad, and other activities, are captured using an IMU sensor worn on the left thigh. The whole work is divided as follows.

1) *Data Collection:* The human gestures data are collected through the IMU sensor embedded with the Arduino Nano 33 BLE sensor board. The data are collected at the sampling frequency data of 110 Hz. The BLE is used to transmit data to the computer system.
2) *Design of Deep Learning Model:* The model is designed over the private data collected with the help of IMU sensor. A hybrid model is developed with the help of MHCNLS. The developed model is again tested over the other benchmark datasets.
3) *Optimization of Model:* To support edge computing, it is necessary to reduce the size of the model to support small size and low power. The compression is done using pruning and quantization. The key advantage is low-powered utilization while preserving the privacy of patient data.
4) *Performance Analysis:* To compare the superiority of the proposed MHCNLS model over various datasets, the performance of the model is compared based on various matrices: F1-score, recall, precision, and accuracy. The confusion matrix is designed to analyze the performance.
5) *Deployment Over Edge Device:* The Aurdino Nano BLE sensor 33 board is used for deployment. The recognized gesture along with the probability by the board is transmitted via color on the board.

B. Organization of This Article

This article is organized into five sections as follows. Section II provides a review of recent state-of-the-art research on HAR. Section III covers the description of private and public datasets, various prepossessing steps, evaluation matrix, and algorithm. Section IV presents the results and discussion, demonstrating the superiority of the MHCNLS model across different datasets. Finally, Section V concludes this article and outlines directions for future work.

II. Literature Review

A significant amount of study has been done in the area of HAR. Here, in this section, all the recent activity recognition works based on the wearable sensor are presented for the survey. Various researchers and scientists across the world are working on the problem of elderly care and wellness monitoring, and body posture and walking activity tracking [15], [16], [17]. Researchers are utilizing various physiological signal analyses for the diagnosis of many motion-related diseases such as multiple sclerosis, Parkinson's, and cerebral palsy at early stages [18], [19], [20]. Challa et al. [21] have proposed a novel multibranch CNN-GRU-based deep learning model for HAR activity classification. They have used various other deep learning models such as CNN, LSTM, and GRU for performance analysis over various public datasets, WISDM, PAMP2, and so on. Since the model has been developed but due to bulk size data how could it become possible to use in real time. Pooja et al. [22], in their research, presented the comprehensive work for the design of the HAR system using a hybrid deep learning model based on multibranched CNN-BiLSTM-BiGRU on various public datasets. However, their work does not consider the spatiotemporal nature of data and the stability of the model.

TABLE I
REVIEW OF STUDIES WITH IMU SENSORS; MEASUREMENT SYSTEMS AND THEIR PERFORMANCE WITH ML TECHNIQUES AND CLASSIFIER

Reference	*IMU Sensor Type*	*No. of Subjects*	*# Activites Types*	*Activities Classifiers*	*Accuracy (%)*
Yi, Myung-Kyu [35] (2023)	Smart Phone Wearable Device	20	Walking, jogging, standing walking upstairs & downstairs	RF+CNN RF-PQ-CNN	94.5 94.4
Semwal et al. [36] (2024)	Arduino nano 33 BLE Sense 9-D IMU	-	WISDM data set HEAHL-HAR dataset	multi-input CNN-LSTM multi-input CNN-LSTM	99.23 98.99
W. Li (2023) [12]	Millimeter-wave Radar	6	Bend, Get down, Stand, Walk, Run, Crawl	DRCNet Vgg-16 DarkNet-19 ResNet-18 AlexNet Lenet-5	93.00 84.67 89.33 88.67 78.33 73.33
Zhou (2022) [13]	Meta MotionR Triaxial accelerometer	8 2,511, 189 samples	Sit, stand, walk briskly, go upstairs, go downstairs, walk slowly, jog and run briskly	CNRENW RNDN CNREDN:	83.4 84.7 83.6
Yang (2022) [14]	Tea Captive T-Sens motion 3-axis accelerometer, gyroscope, & magnetometer	10 subjects 6 activities	Lying, Running, Sitting, Skipping, Standing and Walking	LSTM	99.20
Kwon and Choi (2018)	Smartwatch	2	11 Different Activities	ANN RF	95.0 92.5
De Leonardis et al. (2018)	Xsens MTx	15	Sitting, Standing, Lying Down, Walking, Ascending Descending Stairs, and Uphill and Downhill Walking	kNN MLP SVM Naive Bayes (NB) Decision Tree (DT)	93.4 90.7 91.9 91.5 86.0
Anguita et al. (2012)	Smartphones	30	Walking, Upstairs, Downstairs, Standing, Sitting, Laying	SVM	89.3
He and Jin (2009)	ADXL330 Triaxial Acc.	11 (9M, 2F)	Running, Jumping, Walking, Still	SVM	97.5
Krishnan et al. (2008)	ADXL210E Dual-axial Acc.	10	Walking, Standing, Sitting, Running, Lying Down, Bicycling, Climbing Stairs	AdaBoost RLogReg SVM	92.8 86.6 82.3
Pirttikangas et al. (2006)	Triaxial accelerometer	13 (9M, 4F)	Typing, Watching TV, Drinking, Stairs Ascent and Descent	Multilayer Perceptrons (MLP) KNN	89.8 92.9

CNRENW:Convolutional recurrent network, CNREDN: Convolutional recurrent deep network, RNDN: Recurrent deep network, ANN: Artificial Neural Network.

The researchers have also presented the low-cost IMU-based portable activities recognition system for health care, sports, and medical diagnosis. Bijalwan et al. [23] have proposed wearable sensor-based human activity monitoring for elderly subject health monitoring. They have used an IMU-based wearable sensor, placed on both legs, and captured data for six categories squad, jump, run, stair up and down, and ramp up and down. They have proposed the hybrid deep learning model CNN-LSTM, CNN-GRU, and so on and achieved 96% accuracy. However, the suggested model is inaccurate and it is difficult to wear clinical environment. Soni et al. [17] have proposed the ELM-based generic solution to classify walking into slow, fast, with toes, on heels, stairs ascending, and stairs descending. The developed algorithm ELM performance is compared with SVM and KNN algorithms. Semwal et al. [24] have developed a novel ensemble deep learning model neural network model for lower extremity HAR and planned the trajectories for hip, knee, and ankle joints. The study does not provide a generic and automatic framework for activity recognition.

The HAR also helps people with upper body posture rehabilitation. Wolff et al. [25] have developed different deep learning models, bidirectional long short-time memory (BiLSTM) and CNN. For upper body posture recognition following a stroke, use the CNN-LSTM model. An IMU sensor was used to gather data from 30 people, 19 of whom were male and 11 of whom were female, spanning a range of ages from 10 to 40. Nevertheless, their investigation did not generate or analyze any new data. One of the difficult jobs in HAR is standardizing the data. They have only utilized personal information intended for testing. The primary goal of the proposed hybrid CNN-BiLSTM is to extract features from raw sensor data with as little preprocessing as possible. Various other researchers also developed the HAR system based on deep learning for elderly person tracking system, and their activity recognition system so any fetal accident can be avoided during day-to-day activities [26], [27], [28], [29], [30], [31]. Table I presents the review of various IMU sensor-based HAR systems designed over various machine learning (ML) models.

III. METHODOLOGY

The methodology is divided into five sections, which contain datasets and subjects description, preprocessing of data, deep learning model description, discussion of the proposed model framework, and evaluation and stability of results. Fig. 2 shows the detailed methodology of our work.

A. Problem Statement

The deep learning model sometimes faces the problem of overfitting and underfitting in training data and also at the time to capture the underlying pattern. Striking the right balance to achieve good generalization is a common challenge. Also,

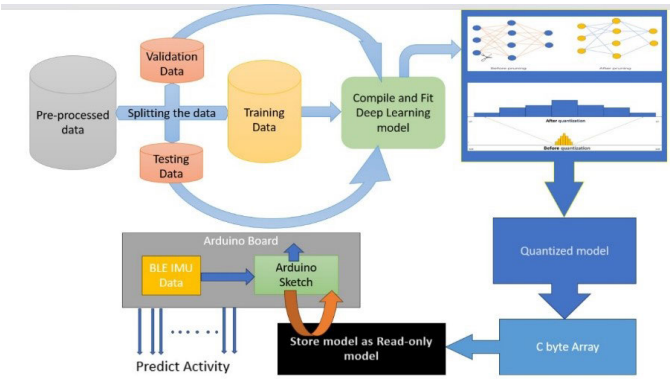

Fig. 2. Flowchart of the proposed methodology.

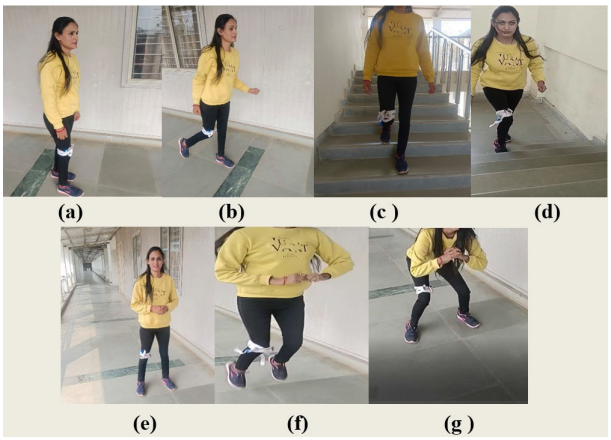

Fig. 3. Data collection of various gestures (a) walk, (b) run, (c) stair-down, (d) stair-up, (e) stand, (f) jump, and (g) sqash, using IMU.

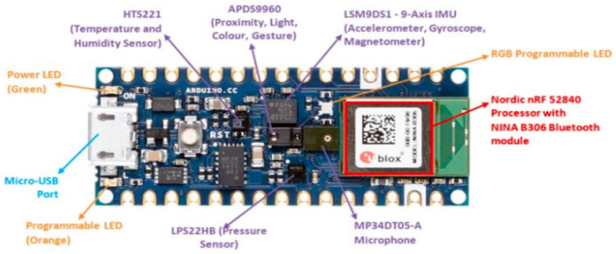

Fig. 4. Physical design of Arduino Nano 33 BLE sense microcontroller.

a lack of interoperability can be a barrier in critical applications where transparency is essential. The models are trained on sensitive data that may inadvertently leak information. Ensuring privacy, especially in significant areas, is a major concern. Ensuring the stability of the deep learning model is also a challenging problem.

B. Leverage of Suggested Method Over Existing Method

The work to recognize different activities related to the lower limb can be utilized to analyze the biomechanics, neuromuscular, and health analysis of different subjects. The noninvasive procedure based on inertial measurement unit (IMU) sensors will help in accessing daily activity, physiological parameters, and health dynamics. Furthermore, to support edge computing, the modern microcontroller equipped with various sensors will be used for computing. The various deep learning models will be fused on microcontrollers using the tinML model by compressing the model from tensor flow lite.

C. Datasets and Subjects Description

This section presents the study and analysis of various HAR datasets, which include physical activities of day-to-day and body motion based on the various wearable sensors. A total of four categories of HAR datasets are utilized in this research.

1) Private Dataset (HEAHL-HAR Dataset): The first dataset is developed by us using Arduino Nano 33 BLE sense-based IMU Sensor at Human Ergonomic, Assistive and Haptic Lab of MANIT Bhopal. A total of 20 healthy subjects participated in data collection. Out of 20 subjects, 15 were male and 5 were female subjects. Table II presents the general description of a private dataset named HEAHL-HAR captured by us. The five gestures, namely, jump, walk, run, squad, and others, are considered for analysis. Fig. 3 shows the visual of various gestures performed by subjects, namely, (a) walk, (b) run, (c) stair-down, (d) stair-up, (e) stand, (f) jump, and (g) sqash. All gestures are collected through a wearable nine-axial IMU sensor worn at the left thigh. Through this data is tuned over various sampling frequencies ranging from 30, 50, 70, 90, 130, and 110 Hz. However, in this research, the frequency of 110 Hz is considered due to the average sample size. For each gesture, the data sample is obtained in 110 data points/sample. Each gesture activity is performed 50 times for different subjects. The next dataset is WISDM.

TABLE II
GENERAL DESCRIPTION OF THE HEAHL-HAR DATASET

Parameter	*Value*
Age	50±15
Weight	50±10
Height	5±.6
Ethnicity	Indian (Asian)
Timing	pre-lunch IST.
Sensor	Six axial IMU sensor.

TABLE III
CLASS DISTRIBUTION OF WISDM DATASET

Name of Activity class	*Sample Size*	*Sample Percentage(%)*
Walking	4,24,400	38.6%
Jogging	342,177	31.2%
Upstairs	1,22,869	11.2%
Downstairs	100,427	9.1%
Sitting	59,939	5.5%
Standing	48,395	4.4%

2) WISDM Dataset: This is a public dataset prepared by the WISDM group and captured using a smartphone placed on the front leg pocket. This dataset includes a total of six categories of gestures walking, jogging, moving upstairs, moving downstairs, sitting, and standing. The sampling frequency of the accelerometer sensors was 20 Hz. Table III presents the subject-wise distribution of WISDM dataset for each activity. In addition, Fig. 5 shows a visual description of WISDM dataset.

3) PAMAP2 Dataset: PAMAP2 data refer to the physical activity monitoring dataset of 18 different gestures performed by nine subjects using three colibri pervasive wireless

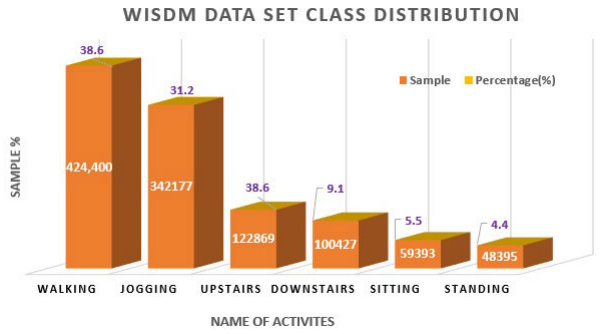

Fig. 5. Class distribution of WISDM dataset.

TABLE IV
GENERAL DESCRIPTION OF PAMAP2 DATASET

Parameter	*Value*
Subjects	9
Gestures	18
Sampling Frequency	110
No. of sensor	3 Colibri wireless accelerometer
HR monitor sampling frequency	9Hz
Sensor's position	wrist on the dominant arm, chest and dominant side's ankle .

accelerometer sensors on 100-Hz sampling frequency. It offers essential information about detecting physical activity and keeping track of health. The dataset is useful for both personal health monitoring and HAR. Three sensors are positioned: one on the chest, one on the dominant side's ankle, and one over the dominant arm's wrist. The sampling frequency used for the heart rate (HR) monitor was 9 Hz. The PAMAP2 data set's overall description is displayed in Fig. 5. Table IV provides a general description of the PAMAP2 dataset.

4) UCI-HAR Dataset: The following six categories have data from UCI-HAR: sitting, standing, laying, walking, walking upstair, and walking downstair. Thirty subjects provide the dataset using a smartphone around their waists to engage in various activities. The accelerometer and gyroscope on the smartphone are used to record the data. The purpose of video recording this experiment was to hand label the data.

D. Preprocessing Steps

The signal captured using the IMU sensor is processed using filters to remove noise and sampled using fixed-size sliding windows of 1.56 s and 50% overlap (128 readings/window). To separate the accelerometer signal reading, a Butterworth low-pass filter is used to separate the gravitational and spatial components of the accelerometer signal. The gravitational signal is considered, a low-frequency component so the cutoff frequency is fixed at 0.2 Hz.

The inaccurate placement of the sensor may result in wrong measurements obtained from the sensor due to the addition of noise. Therefore, the preprocessing of raw recorded sensor data is important before feeding to classifier [32]. Data normalization is the process of adjusting the range of data in your dataset to a common scale, especially to improve the performance and stability of deep learning algorithms. Here, we have used min–max normalization. It scales the data to a fixed range, typically [0, 1]. Equation (1) shows the formula of min–max normalization, where $X_{\max}$ is the maximum value of x and $X_{\min}$ is the minimum value of x

$$X_{\text{norm}} = \frac{x - x_{\min}}{X_{\max} - X_{\min}}. \tag{1}$$

The idea of normalized convolution (NC), which is predicated on the theory of confidence-equipped signals, restores invalid measurements of data [33]. Let the tainted input with the confidence be the discrete signal $f(\boldsymbol{x})$, whether each discrete sample is legitimate or invalid, be represented by $m(\boldsymbol{x})$. To express the coordinate position within an image, use the variable $\boldsymbol{x} = (x, y)$. It is simple to determine the confidence $m(\boldsymbol{x})$ for a saturated or overexposed sensor sample. By verifying that there are no zero entries in the values, the Kinect sensor can provide the confidence of each pixel in $g(\boldsymbol{x})$. The neighborhood is represented by the polygon ω_x, whose center is at x and whose size is $(2r+1)^2$. Equation (2) can be used to retrieve the restored and denoised signal $r(\mathbf{x})$ of the invalid depth measurement

$$r_{\text{NC}}(x) = \frac{\sum_{\epsilon\omega_x} g(x')a(x,x')m(x')}{\sum_{\epsilon\omega_x} a(x,x')m(x')} \tag{2}$$

$$a(x,x') = \exp\left(-\frac{\|x-x'\|^2}{{\sigma_s}^2}\right) \tag{3}$$

where the applicability function $a(x, x')$ has a pdf of Gaussian nature and σ_s represents the spatial similarity.

As only invalid data points are restored, hence, actual filter may be represented as follows:

$$\tilde{r}_{\text{NC}}(x) = f(x)m(x) + r_{\text{NC}}(x)(1 - m(x)). \tag{4}$$

Following the recovery of incorrect data, the entire dataset is scaled and normalized. The approach of nonapproximative guided filtering is utilized in order to maintain the edges [34].

E. Hybrid Deep Learning Model

1) CNN-LSTM (CNLS): The hybrid deep learning model CNN-LSTM is often used to address tasks that involve both spatial and temporal dependencies, such as video analysis or sequential data processing. The input data, which could be spatiotemporal, are initially processed by the CNN to capture spatial features. The output from the last convolutional layer serves as a set of features that represent the spatial information for the next layer. The output from the CNN is then fed into the LSTM layers, where the temporal dependencies are modeled. The LSTM is capable of learning patterns and relationships over time and integrating the spatial features obtained from the CNN. The combination of CNN and LSTM leverages the strengths of CNNs in spatial feature extraction and LSTMs in modeling sequential dependencies. This architecture is effective for tasks where both spatial information and temporal information are crucial, such as action recognition in videos or time series forecasting.

2) CNN-GRU (CNGR): The other hybrid CNN-GRU model is a powerful architecture that leverages the strengths of CNNs for spatial feature extraction and GRUs for sequential modeling. The output from the CNN is then fed into the GRU

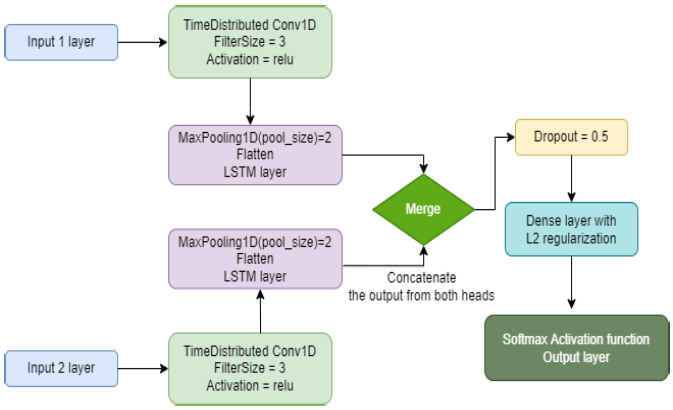

Fig. 6. Layer representation of the proposed multiheaded CNN-LSTM model.

TABLE V
MODEL ARCHITECTURE

Layer type	*Output shape*	*No. of parameters*
Input Layer (CNN)	(None, 256, 4)	0
$Conv1D_1$	(None, 254, 32)	416
$MaxPooling1D_1$	(None, 127, 32)	0
$Dropout_1$	(None, 127, 32)	0
$Conv1D_2$	(None, 125, 64)	6208
$MaxPooling1D_2$	(None, 62, 64)	0
$Dropout_1$	(None, 62, 64)	0
Flatten (CNN)	(None, 3968)	0
Input Layer (LSTM)	(None, 256, 4)	0
$LSTM_1$	(None, 256, 32)	4736
$LSTM_2$	(None, 16)	3136
Concatenate	(None, 3984)	0
Dense	(None, 32)	127520
Dense	(None, 3)	99

layers. The GRU model processes this spatial information sequentially, capturing temporal dependencies and patterns over time. The sequential modeling provided by GRUs allows the model to understand the temporal evolution of features extracted by CNN. GRUs are useful for tasks where understanding the order of input elements is important. GRUs use two gates upset and reset that allow them to selectively update their memory cell and control information flowthrough the network. This makes GRUs capture long-term dependencies in sequential data that are more efficient than other traditional deep learning models.

3) Proposed Multiheaded CNN-LSTM (MHCNLS): The multiheaded attention mechanism is applied to the combined output of the CNN and LSTM. Each attention head focuses on different aspects of the feature representation, allowing the model to attend to various spatial and temporal patterns. The multiheaded CNN-LSTM model integrates spatial and sequential processing through CNN and LSTM components, respectively, and employs a multiheaded attention mechanism to focus on different aspects of the input data. The architecture is very effective for tasks that require capturing both spatial and temporal dependencies with the ability to selectively attend to different parts of the input. The multiheaded attention mechanism allows the model to focus on different parts of the input data with multiple attention heads. The attention mechanism is applied to the output of the CNN and LSTM components. Each attention head attends to a different aspect of the features, enabling the model to selectively weigh the importance of different spatial or temporal elements. The outputs from the attention heads are typically concatenated or combined in some way. Fig. 6 shows the layer representation of the proposed multiheaded CNN-LSTM (MHCNLS) model. Table V shows the layer-wise model architecture and parameter list.

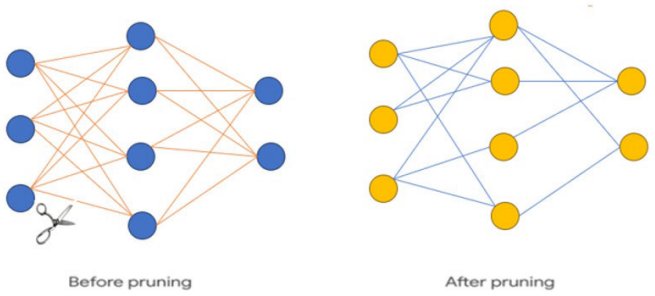

Fig. 7. Process of model pruning.

4) Model Pruning and Quantization: Model pruning and quantization are techniques used to optimize deep learning models for deployment on resource-constrained devices. They enable the creation of more efficient and lightweight models without significantly compromising their performance, making them well suited for real-world applications in various domains, also making them more efficient in terms of storage, memory, and computation. These techniques are particularly useful for deploying models on resource-constrained devices, such as mobile devices or edge devices. The Audrina Nano 33 BLE has about 1 MB of storage space about which 600 kB is usable. For using our developed model in real-time working, it is needed to reduce the size of the model, so we can embed it in our preferred microcontroller. Figs. 7 and 8 show the model pruning and quantization process from visulation. Pruning is an iterative process on a trained model that trims insignificant weights by setting those weights to zero until the specified target sparsity. Remove unnecessary connections between the layers. It reduces the model size and power consumption and also executes quickly, while model quantization involves representing weights with fewer bits, typically 8 bits or fewer, instead of the standard 32 bits used in most deep learning frameworks. Equation (5) representation of the conversion of float value into int8

$$\left\{\begin{array}{c} \text{Quantized}_{\text{value}} = \dfrac{\text{float}_{\text{value}}}{\text{scale}} + \text{zero}_{\text{point}} \\ \text{Where: scale} = \dfrac{(\max - \min)}{2^{\text{bits}}} \\ \{\text{Floating point size of each bin}\} \\ \text{zero}_{\text{point}}\text{:}\{\text{integer zero corresponding to floating point zero}\} \end{array}\right\}. \tag{5}$$

F. Hardware Platform and Performance Index

1) Hardware and Software Simulation Environment: The Arduino Nano 33 BLE sense board is used for data collection. The detailed specification of the board is listed in Table VI.

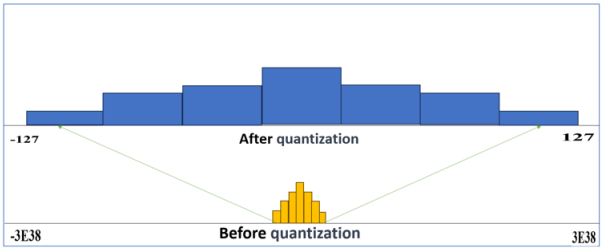

Fig. 8. Process of model quantization.

Algorithm 1 Proposed Multiheaded CNN-LSTM (MHCNLS)-Based HAR Algorithm

Calculate the Performance Metrics Such as Accuracy, Precision, Recall, and F1-Score for Different Activities **Input**: Raw signal data of accelerometer and gyroscope reading $a1_x, a2_x, a3_x, g1_x, g2_x, g3_x$
Output: classification results of compressed deep learning model **Procedure:**

Step 1: Capture the raw signal data using 6 degrees of IMU sensor.

1) accelerometer reading $a1_x, a2_x, a3_x$
2) gyroscope reading: $g1_x, g2_x, g3_x$

Step 2: Reprocess data:

1) removal of noise by applying the filter.
2) sampled using fixed-size sliding windows.
3) Butterworth low-pass filter to separate the gravitational and spatial components of the accelerometer signal.

Step 3: Prepare the dataset by dividing it into training, validation, and testing sets.
Step 4: Apply the proposed MPCNLS deep learning model for model training
Step 5: Repeat step 4 until the error can not reduced significantly
Step 6: Results and performance analysis:
6.1 Classification accuracy, F1_score, precision and recall values of different gesture using.

$$\left\{\begin{array}{c} Accuracy = \frac{TP+TN}{TP+TN+FP+FN} \\ \textbf{where: TP: true positive,TN: true negative,} \\ \textbf{FP: false positive \& FN: false negative;} \end{array}\right\} \quad (6)$$

6.2 Apply pruning and quantization using eq. 5 to reduce the model size to fuse on edge device.
Step 7: Compare results with various other deep learning models CNN-LSTM(CNLS), CNN-GRU(CNGR), Multi-branch CNN-LSTM(MBCNLS), CNN-BiLSTM(CNBiLS) & multi-headed CNN-LSTM (MHCNLS);

The Python simulations were performed using Google Colab, which provides GPU for parallel computing; the computer system was used based on *Microsoft Windows 11 with an Intel Core i5 processor and CPU clocked at 3.40 GHz, 32 GB of RAM, and a chipset of 2600.* Fig. 8 shows the physical design of Arduino Nano 33 BLE sense microcontroller. It consists of nine onboard sensors. Here, in research, the LSM9D51 nine-axis IMU sensor is used.

TABLE VI
SPECIFICATION SHEET OF ARDUINO NANO 33 BLE SENSE BOARD

Parameter	*Value*
Form factor	45x18mm dimensions
Processor	Nordic nRF52840
CPU	32-bit ARM Cortex M4
Flash Memory	1MB
Operating Voltage	3.3V
Communication interface Bluetooth low energy (BLE)	NINA B306 module
SRAM	256KB
No. of sensor	9 on board sensors

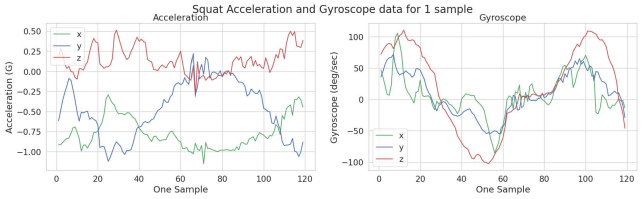

Fig. 9. Squat acceleration and gyroscope data for one sample.

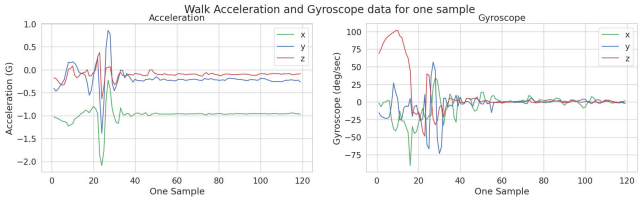

Fig. 10. Walk acceleration and gyroscope data for (a) one sample and (b) three samples.

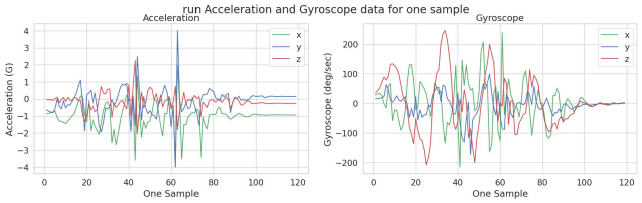

Fig. 11. Running acceleration and gyroscope data for one sample.

2) Performance Matrix: The performance of the proposed model MHCNLS will be compared based on the accuracy (%) = (TP + TN)/(TP + TN + FP + FN), precision (P) = (TP/(TP + FP)), recall (R) = (TP/(TP + FN)), F1-score = $(2 * P * R)/(P + R)$ = $(2 * \mathrm{TP})/(2 * \mathrm{TP} + \mathrm{FP} + \mathrm{FN})$, specificity ($S_p$) = (TP/(TP + FN)), and sensitivity (S) = (TN/(FP + TN)), where TP, TN, FP, and FN stand for true positive, true negative, false positive, and false negative, respectively. All the above values can be calculated after preparing the confusion matrix.

G. Proposed Algorithm

Algorithm 1 shows the proposed MPCNLS algorithm for gesture classification. In Algorithm 1 taken HEAHL-HAR, WISDM, PAMP2, UCI-HAR dataset as input source and reported out in terms of F1-score, precision, classification accuracy, and recall given in Section III-F2. The accelerometer signal readings are represented using a_x, a_y, and a_z; gyroscope

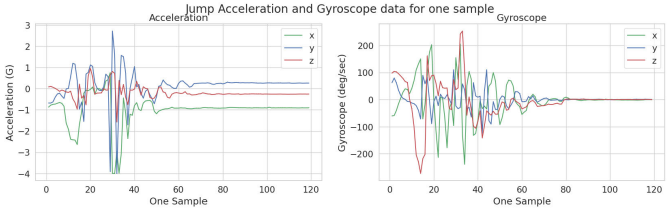

Fig. 12. Jump acceleration and gyroscope data for one sample.

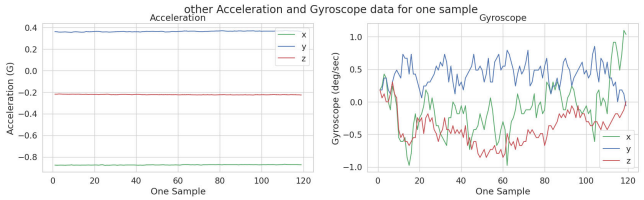

Fig. 13. Any other gesture acceleration and gyroscope data for one sample.

TABLE VII
METRICS SHOWING COMBINED RESULTS

Dataset	Model	A	P	R	F1-Score
	CNLS	92.65	90.41	92.21	92.12
	CNGR	91.19	90.60	90.09	89.94
HEAH-	MBCNLS	94.43	92.64	93.21	94.18
HAR	CNBiLS	93.56	91.24	92.43	92.61
	MHCNLS	***98.17***	***96.20***	***95.91***	***96.21***
	CNLS	93.76	91.04	92.14	91.43
	CNGR	92.83	90.38	92.01	91.14
WISDM	MBCNLS	94.41	93.11	93.86	94.15
	CNBiLS	92.47	89.80	93.59	91.78
	MHCNLS	***96.25***	***95.56***	***95.71***	***95.91***
	CNLS)	91.04	89.76	88.34	91.53
	CNGR	88.38	87.83	87.01	88.14
PAMP2	MBCNLS	91.61	90.14	91.78	92.75
	CNBiLS	82.47	74.80	63.59	61.78
	MHCNLS	***97.67***	***97.30***	***97.91***	***97.56***
	CNLS	92.16	95.42	92.94	91.98
	CNGR	88.83	88.38	87.01	87.14
UCI-HAR	MBCNLS	89.61	88.11	88.86	86.65
	CNBiLS	85.17	84.11	84.55	83.18
	MHCNLS	***95.73***	***97.10***	***96.83***	***96.11***

where, CNLS:CNN-LSTM, CNGR: CNN-GRU, CNBiLS: CNN-BiLSTM, BCNLS: Multibranch CNN-LSTM,***MHCNLS: Multiheaded CNN-LSTM***. A:Accuracy, P:Precision, R: Recall

readings are represented using g_x, g_y, and g_z; and m_x, m_y, and m_z are the magnetometer readings.

IV. RESULTS AND DISCUSSION

A. Interpretation of Different Gesture Movement Plots

In this research, five gestures, namely, jump, walk, run, squad, and others, are considered for neuromuscular analysis. All gestures are collected through a wearable 6-DoF IMU sensor worn at the left thigh. Through this, data are tuned over various sampling frequencies ranging from 20, 40, 60, 250, and 110 Hz. However, in this research, the frequency of 110 Hz is considered due to the average sample size. For each gesture, the data sample is obtained in 110 data points/sample. Each gesture activity is performed 50 times for different subjects. Figs. 9–13 show the visualization of the gestures sample data of squad, walk, run, jump, and others, respectively.

TABLE VIII
COMPARATIVE RESULTS OF DIFFERENT MODELS

Model	*A*	*P*	*F1 Score*	*S*	*Sp*
CNLS	92.40	92.82	73.2	93.1	94.48
CNGR	90.30	54.78	65.12	80.28	94.03
MBCNLS	92.51	68.35	76.92	87.94	96.33
CNBiLS	88.42	63.33	72.16	83.85	95.62
MHCNLS	96.95	54.13	64.84	80.84	93.8

where, A=Accuracy, P=Precision, S= Sensitivity, $S_p = Specificity$.

TABLE IX
COMPARISON OF OUR PROPOSED METHODOLOGY WITH THE EXISTING MODELS

References	*Dataset*	*Model*	*A*
Sain (2023) [6]	WISDM	CNBILSGR	97.12
Nidhi (2021) [7]	WISDM	INCNGR	97.47
Sravan (2022) [8]	WISDM	MBCNBILS	96.83
Neha (2023) [11]	PAMP2	CNN-LSTM	97.38
Proposed model	WISDM,	MBCNLS(Proposed)	96.25
	HEAHL-HAR	MBCNLS(Proposed)	98.17

where, A=Accuracy, CNBILSGR:ConvBiLSTM-GRU, INCNGR: Inception CNN-GRU, MBCNBILS: Multiibranch CNN-BiLSTM, MBCNLS: Multi-branch CNN-LST.

TABLE X
MATRICES SHOWING INDIVIDUAL ACTIVITY RESULTS

Model	Parameters	Gestures				
		Walk	Run	Jump	Squad	Other activities
MBCNLS	Accuracy	0.97	1	0.95	0.96	1
	Precision	1.0	1.0	0.98	0.97	0.98
	Recall	0.97	1.0	0.98	0.96	1.0
	F1	0.99	1.0	0.97	0.96	0.99
	Support	.97	.98	.96	.97	.98
CNBiLS	Accuracy	0.96	0.97	0.95	0.95	0.96
	Precision	0.98	1.0	0.98	0.97	1.0
	Recall	0.96	0.97	0.98	0.96	0.98
	F1	0.98	0.96	0.96	0.98	0.99
	Support	0.96	0.97	0.98	0.96	0.95
MHCNLS	Accuracy	0.99	0.97	0.99	0.98	0.97
	Precision	0.98	0.99	0.97	0.97	0.99
	Recall	0.98	0.97	0.98	1	0.98
	F1	0.99	1	0.96	0.98	0.99
	Support	0.97	0.97	0.96	0.98	0.98

TABLE XI
PERFORMANCE ANALYSIS OF THE PROPOSED MODEL TO CALCULATE TIME COMPLEXITY ON THE HEAHL-HAR DATASET

Performance	*Methods*				
	CNLS	*CNGR*	*MBCNLS*	*CNBiLS*	*MHCNLS*
Training time(s)	4.12	4.17	4.12	4.22	4.25
Testing time(ms)	256.9	328.6	353.4	278.3	242.8
Testing accuracy(%)	92.40	90.30	92.51	88.42	96.95

1) Interpretation of Fig. 9: It becomes evident from the above plot of the accelerometer on the x-, y-, and z-axis that the range of acceleration is -1.00- to 0.50-g force, which shows not many jerks and single peaks, and it is continuous movement in all three directions. Similarly, the gyroscope shows a sinusoidal pattern-type curve for all three directions. It shows that all three joints, hip, knee, and ankle, are not getting any major thrust, and movement is well planned.

2) Interpretation of Fig. 10: The walking plot for the one and three samples clearly shows that during initial contact when heel strike is taking place, the maximum jerk is observed between -2.0 and 1.0 for the left leg as a person is right-handed, whereas in the right leg, the jerk accelerates in a

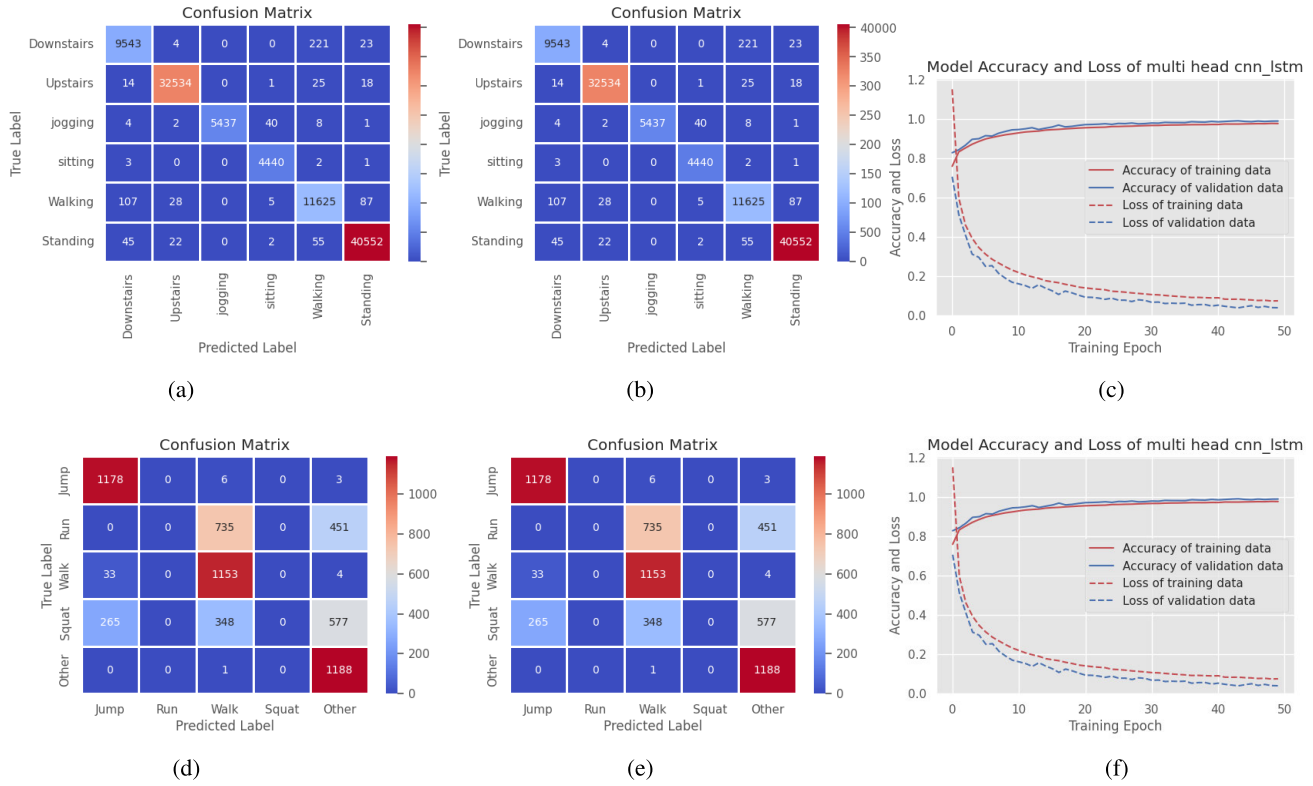

Fig. 14. Confusion matrix and accuracy curve of various models. (a) Confusion matrix for CNN-LSTM for WISDM. (b) Confusion matrix for multiheaded CNN-LSTM for WISDM. (c) Accuracy and error curve for simple model UCI HAR. (d) Confusion matrix for multiheaded CNN-LSTM for private. (e) Confusion matrix for CNN-LSTN for private. (f) Accuracy and error curve for simple model UCI HAR.

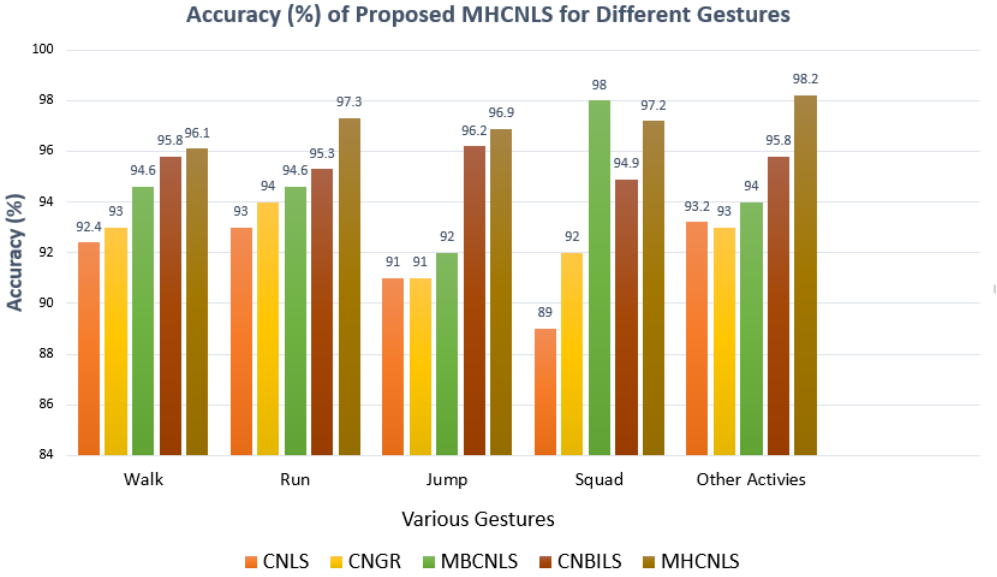

Fig. 15. Accuracy % of the proposed MHCNLS for different gestures.

positive direction between −1.0 and 1.0 and deceleration is less since the impact is less due to the right-hand position. Similarly, if a person is left-handed, the behavior of the plot will be just vice versa. The major events during walking are heel strike, toe-off, and knee bend. From the figure, it is clear that the behavior is vice versa and depends on the working hand position. As neurological, the right lobe of the brain is more active for a right-hand person, which results in more jerk or pressure on the right leg and vice versa. The walking is best exercise for cardiovascular and pulmonary disease and does not have a very adverse impact on different body joints in the long run.

3) Interpretation of Fig. 11: The gesture running results in maximum impact all the during of running. The range of accelerometer id −4 to 4 in both directions impact is more continuous and rotation is −200 to +200 rotation/s. Due to the high impact all the time, the trajectories of running require careful planning, so the jerk can observe, so the least damage

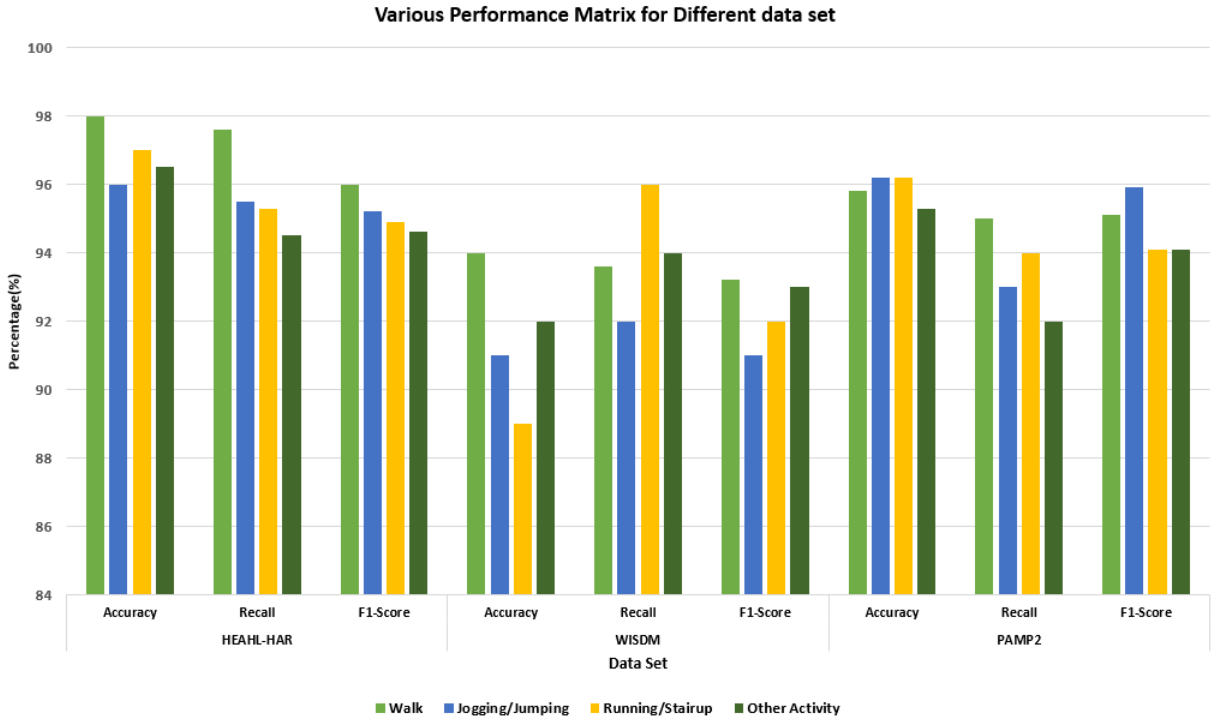

Fig. 16. Performance analysis of the proposed MHCNLS for different gestures across HEAL-HAR, WISDM, and PAMAP2 datasets.

TABLE XII
AVERAGE PRECISION, RECALL, AND F1_SCORE OBTAINED OF EACH HEALTHY SUBJECT FOR EACH ACTIVITY

Subject	Accuracy			Precision			Recall			F1_score		
	Walking	**Standing**	**Sitting**	**Walking**	**Standing**	**Sitting**	**Walking**	**Standing**	**Sitting**	**Walking**	**Standing**	**Sitting**
1	100±0	99.2±1.4	100±0	100±0	100±0	99.1±1.5	100±0	99.6±0.7	99.6±0.8	100±0	99.2±1.4	100±0
2	100±0.0	100±0	99.1±1.5	100±0	99.2±1.4	100±0	100±0	99.6±0.7	99.6±0.8	100±0.0	100±0	99.1±1.5
3	98.4±1.8	97.8±3.8	98.5±2.6	99.2±1.4	99.2±0.7	94.7±9.2	98.8±1.6	96.5±2.1	98.5±6.1	98.4±1.8	97.8±3.8	98.5±2.6
4	100±0.0	97.3±4.6	98.6±2.5	98.3±3	99.6±0.7	97.7±4.0	99.1±1.5	98.1±2.7	98.4±3.3	100±0.0	97.3±4.6	98.6±2.5
5	99.1±1.6	99.1±1.6	98.7±1.2	98.6±1.4	99.5±0.8	98.7±2.2	98.8±1.1	98.7±1.2	99.3±1.3	99.1±1.6	99.1±1.6	98.7±1.2
6	99.7±0.6	97.4±4.5	99.6±0.8	98.3±3	100±0	97.5±3.3	98.9±1.4	98.5±2.3	98.7±2.1	99.7±0.6	97.4±4.5	99.6±0.8
7	100.0±0	98.0±0.5	98.0±2.4	100.0±0	98.6±1.8	97.2±0.7	100.0±0	98.3±0.9	97.6±1.2	100.0±0	98.0±0.5	98.0±2.4
8	99.7±0.5	99.5±0.9	96±7	97.1±5.1	99.2±1.4	99.7±0.6	98.4±2.9	97.7±1.1	99.3±4.0	99.7±0.5	99.5±0.9	96±7
9	98.8±2.0	99.7±0.5	98.9±1.9	98.5±1.8	99.1±1.6	99.7±0.5	98.7±1.9	99.3±0.7	99.4±1.2	98.8±2.0	99.7±0.5	98.9±1.9
10	100±0	99.8±0.4	99.5±0.5	100±0	99.3±0.7	99.8±0.3	100±0	99.7±0.4	99.6±0.3	100±0	99.8 ±0.4	99.5 ± 0.5
11	99.3 ± 1.3	100.0 ± 0	98.8 ± 2.0	100.0 ± 0	98.5 ± 2.6	100.0 ± 0	99.6 ± 0.6	99.2 ± 1.3	99.4 ± 1.0	99.3 ± 1.3	100.0 ± 0	98.8 ± 2.0
Average	**99.5 ± 0.7**	**98.6 ± 1.5**	**98.8 ± 2.0**	**99.0 ± 1.4**	**99.5 ± 1.1**	**97.9 ± 2.2**	**99.3 ± 1.0**	**98.4 ± 1.3**	**99.0 ± 2.0**	**99.5 ± 0.7**	**98.6 ± 1.5**	**98.8 ± 2.0**

can be beard by the robot on knee joint or a human being. Due to this in a later stage, the knee replacement and knee impairment problem a person faces results in abnormality in gait behavior.

4) Interpretation of Fig. 12: The jump gesture clearly shows a single point highest peak when, after the jump, the foot strikes on ground. The single peak value is observed to have a range of −4 to 3, which is also significant and requires careful planning of trajectory. Three joints, hip, knee, and ankle, are not getting any major thrust, and movement is well planned.

5) Interpretation of Fig. 13: Any other activity considers the static gesture, so it has very less impact on health, and the accelerometer and gyroscope both give a very normal range.

B. Result Description

The proposed model is tested over all four datasets, namely, HEAHL-HAR, WISDM, PAMP2, and UCI-HAR. The results are reported based on model performance listed in Table VII. The proposed model MHCNLS has shown consistently better results on all the datasets. Table VIII shows the average performance of all models over different datasets. Fig. 14(a) shows the comparison of our proposed methodology with the existing literature of artwork models. Fig. 14(a), (b), (d), and (e) shows the confusion matrix for WISDM and private HEAHL-HAR dataset using MHCNLS and CNLS model, whereas Fig. 14(a), (c), and (f) shows the accuracy and error curve for the proposed MHCNLS. Table IX compares the proposed MHCNLS model with existing models.

Fig. 15 shows the accuracy % of the proposed MHCNLS for different gestures. Table X shows the accuracy of the proposed MHCNLS model for different activities, namely, walk, run, jump, squad, and other activities. Table XI shows the calculated time complexity on the HEAHL-HAR dataset of various deep learning models. Fig. 16 shows the performance analysis of the proposed MHCNLS for different gestures across HEAL-HAR, WISDM, and PAMAP2 datasets. Table XII presents the performance of different activities for healthy subjects.

V. CONCLUSION AND FUTURE SCOPE

In this research, an autonomous HAR system based on deep learning is proposed. The proposed model, MHCNLS,

has demonstrated superior accuracy across multiple datasets, including WISDM, PAMPM2, UCI-HAR, and a private dataset, HEAHL-HAR. Throughout a variety of tasks, the suggested model has demonstrated the best accuracy. The private dataset HEAHL-HAR is collected using Arduino Nano 33 BLE Sense Board. The captured gestures were jump, walk, squad, run, and other activities. The MHCNLS model achieved an impressive accuracy of 98.17% on the HEAHL-HAR dataset. Comparatively, the model reported accuracies of 96.25%, 97.67%, and 95.73% on the WISDM, PAMPM2, and UCI-HAR datasets, respectively. The performance of the MHCNLS model is also compared with other hybrid deep learning models, CNLS, MBCNLS, CNBiLS, CNGR, and so on. In addition, the size of the deep learning model is significantly reduced almost five times using pruning and quantization, enhancing its suitability to support edge computing and being computationally efficient. The raw signal analysis for one sample is presented. The work has demonstrated that the proposed MHCNLS model has utilized the benefit of spatial and temporal data and outperformed all the previous work.

For future work, we aim to address issues related to dataset standardization and data imbalance and consider larger datasets with additional activities for fall recovery. In addition, the study can include normalization data to zero mean and unit variance, which accelerates the model's convergence and increases its effectiveness. The collection of data was extremely unbalanced, and that aspect had not been taken into account in the earlier studies. In the future, the problem of unbalanced datasets can be addressed to mitigate the issue of data imbalance.

Dataset Source

The dataset used in this study is available in the UCI Machine Learning repository—PAMP2: https://archive.ics.uci.edu/dataset/231/pamap2+physical+activity+monitoring, WISDM: https://archive.ics.uci.edu/dataset/507/wisdm+smartphone+and+smartwatch+activity+and+biometrics+dataset, UCI HAR: https://archive.ics.uci.edu/dataset/240/human+activity+recognition+using+smartphones, and Private: https://archive.ics.uci.edu/dataset/240/human+activity+recognition+using+smartphones.

Acknowledgment

The resource for data collecting was provided by the Human Ergonomic, Assistive and Haptic Lab of MANIT Bhopal, for which the author(s) is grateful. The HEAHL dataset's volunteer participants and the dataset inventor are both thanked by the author(s).

References

[1] N. Gaud, M. Rathore, and U. Suman, "Human gait analysis and activity recognition: A review," in *Proc. IEEE Guwahati Subsection Conf. (GCON)*, Jun. 2023, pp. 1–6.

[2] N. Dua, S. N. Singh, S. K. Challa, V. B. Semwal, and M. L. S. S. Kumar, "A survey on human activity recognition using deep learning techniques and wearable sensor data," in *Proc. Int. Conf. Mach. Learn., Image Process., Netw. Secur. Data Sci.* Bhopal, India: Springer, 2022, pp. 52–71.

[3] V. B. Semwal, R. Jain, P. Maheshwari, and S. Khatwani, "Gait reference trajectory generation at different walking speeds using LSTM and CNN," *Multimedia Tools Appl.*, vol. 82, no. 21, pp. 33401–33419, Sep. 2023.

[4] Y. Li and L. Wang, "Human activity recognition based on residual network and BiLSTM," *Sensors*, vol. 22, no. 2, p. 635, Jan. 2022.

[5] R. Jain, V. B. Semwal, and P. Kaushik, "Stride segmentation of inertial sensor data using statistical methods for different walking activities," *Robotica*, vol. 40, no. 8, pp. 2567–2580, Aug. 2022.

[6] M. K. Sain, J. Singha, S. Saini, and V. B. Semwal, "Human action recognition using ConvBiLSTM-GRU in indoor environment," in *Proc. IEEE Global Conf. Artif. Intell. Internet Things (GCAIoT)*, Dec. 2023, pp. 179–186.

[7] N. Dua, S. N. Singh, V. B. Semwal, and S. K. Challa, "Inception inspired CNN-GRU hybrid network for human activity recognition," *Multimedia Tools Appl.*, vol. 82, no. 4, pp. 5369–5403, Feb. 2023.

[8] D. Bhattacharya, D. Sharma, W. Kim, M. F. Ijaz, and P. K. Singh, "Ensem-HAR: An ensemble deep learning model for smartphone sensor-based human activity recognition for measurement of elderly health monitoring," *Biosensors*, vol. 12, no. 6, p. 393, Jun. 2022.

[9] R. Jain and V. B. Semwal, "A novel feature extraction method for preimpact fall detection system using deep learning and wearable sensors," *IEEE Sensors J.*, vol. 22, no. 23, pp. 22943–22951, Dec. 2022.

[10] V. B. Semwal, A. Kumar, P. Nargesh, and V. Soni, "Tracking of fall detection using IMU sensor: An IoHT application," in *Proc. 3rd Int. Conf. MIND*. Bhopal, India: Springer, 2023, pp. 815–826.

[11] N. Gaud, M. Rathore, and U. Suman, "Hybrid deep learning-based human activity recognition (HAR) using wearable sensors: An edge computing approach," in *Proc. Int. Conf. Data Anal. Manag.* Jalania Gora, Poland: Springer, 2023, pp. 399–410.

[12] W. Li, X. Wu, W. Deng, and Y. Dong, "Human activity recognition of millimeter-wave radar based on DRCNet," in *Proc. IEEE Int. Symp. Antennas Propag. (ISAP)*, Oct. 2023, pp. 1–2.

[13] F. Zhou, R. Wang, H. Su, and S. Xu, "A human activity recognition model based on wearable sensor," in *Proc. 9th Int. Conf. Digit. Home (ICDH)*, Oct. 2022, pp. 169–174.

[14] H. Yang, X. Wen, Y. Geng, Y. Wang, X. Wang, and C. Lu, "MPJA-HAD: A multi-position joint angle dataset for human activity recognition using wearable sensors," in *Proc. Int. Conf. Adv. Mech. Syst. (ICAMechS)*, Dec. 2022, pp. 178–182.

[15] E. Essa and I. R. Abdelmaksoud, "Temporal-channel convolution with self-attention network for human activity recognition using wearable sensors," *Knowl.-Based Syst.*, vol. 278, Oct. 2023, Art. no. 110867.

[16] S. Zhang et al., "Deep learning in human activity recognition with wearable sensors: A review on advances," *Sensors*, vol. 22, no. 4, p. 1476, Feb. 2022.

[17] V. Soni, H. Yadav, V. B. Semwal, B. Roy, D. K. Choubey, and D. K. Mallick, "A novel smartphone-based human activity recognition using deep learning in health care," in *Proc. 3rd Int. Conf. MIND*. Bhopal, India: Springer, 2023, pp. 493–503.

[18] V. Bijalwan, V. B. Semwal, and T. K. Mandal, "Fusion of multi-sensor-based biomechanical gait analysis using vision and wearable sensor," *IEEE Sensors J.*, vol. 21, no. 13, pp. 14213–14220, Jul. 2021.

[19] H. F. Nweke, Y. W. Teh, M. A. Al-garadi, and U. R. Alo, "Deep learning algorithms for human activity recognition using mobile and wearable sensor networks: State of the art and research challenges," *Exp. Syst. Appl.*, vol. 105, pp. 233–261, Sep. 2018.

[20] V. B. Semwal et al., "Development of the LSTM model and universal polynomial equation for all the sub-phases of human gait," *IEEE Sensors J.*, vol. 23, no. 14, pp. 15892–15900, Jul. 2023.

[21] S. K. Challa, A. Kumar, and V. B. Semwal, "A multibranch CNN-BiLSTM model for human activity recognition using wearable sensor data," *Vis. Comput.*, vol. 38, no. 12, pp. 4095–4109, Dec. 2022.

[22] P. Lalwani and G. Ramasamy, "Human activity recognition using a multi-branched CNN-BiLSTM-BiGRU model," *Appl. Soft Comput.*, vol. 154, Mar. 2024, Art. no. 111344.

[23] V. Bijalwan, V. B. Semwal, and V. Gupta, "Wearable sensor-based pattern mining for human activity recognition: Deep learning approach," *Ind. Robot, Int. J. Robot. Res. Appl.*, vol. 49, no. 1, pp. 21–33, Jan. 2022.

[24] V. B. Semwal, N. Gaud, P. Lalwani, V. Bijalwan, and A. K. Alok, "Pattern identification of different human joints for different human walking styles using inertial measurement unit (IMU) sensor," *Artif. Intell. Rev.*, vol. 55, no. 2, pp. 1149–1169, Feb. 2022.

[25] C. Wolff et al., "Effects of age, body height, body weight, body mass index and handgrip strength on the trajectory of the plantar pressure stance-phase curve of the gait cycle," *Frontiers Bioeng. Biotechnol.*, vol. 11, Feb. 2023, Art. no. 1110099.
[26] R. Jain, V. B. Semwal, and P. Kaushik, "Deep ensemble learning approach for lower extremity activities recognition using wearable sensors," *Exp. Syst.*, vol. 39, no. 6, Jul. 2022, Art. no. e12743.
[27] S. K. Challa, A. Kumar, V. B. Semwal, and N. Dua, "An optimized-LSTM and RGB-D sensor-based human gait trajectory generator for bipedal robot walking," *IEEE Sensors J.*, vol. 22, no. 24, pp. 24352–24363, Dec. 2022.
[28] S. K. Challa, A. Kumar, V. B. Semwal, and N. Dua, "An optimized deep learning model for human activity recognition using inertial measurement units," *Exp. Syst.*, vol. 40, no. 10, Dec. 2023, Art. no. e13457.
[29] N. Dua, S. N. Singh, and V. B. Semwal, "Multi-input CNN-GRU based human activity recognition using wearable sensors," *Computing*, vol. 103, no. 7, pp. 1461–1478, Jul. 2021.
[30] E. Warmerdam, C. Hansen, R. Romijnders, M. A. Hobert, J. Welzel, and W. Maetzler, "Full-body mobility data to validate inertial measurement unit algorithms in healthy and neurological cohorts," *Data*, vol. 7, no. 10, p. 136, 2022.
[31] V. B. Semwal, P. Tokas, M. Nilesh, and N. Khare, "Dynamic balancing of bipedal robot on inclined terrain using polynomial trajectories," in *Proc. 7th Int. Conf. Graph. Signal Process.*, Jun. 2023, pp. 72–77.
[32] S. Qiu et al., "Multi-sensor information fusion based on machine learning for real applications in human activity recognition: State-of-the-art and research challenges," *Inf. Fusion*, vol. 80, pp. 241–265, Apr. 2022.
[33] A. Eldesokey, M. Felsberg, and F. S. Khan, "Confidence propagation through CNNs for guided sparse depth regression," *IEEE Trans. Pattern Anal. Mach. Intell.*, vol. 42, no. 10, pp. 2423–2436, Oct. 2020.
[34] K. He, J. Sun, and X. Tang, "Guided image filtering," *IEEE Trans. Pattern Anal. Mach. Intell.*, vol. 35, no. 6, pp. 1397–1409, Jun. 2013.
[35] M.-K. Yi, W.-K. Lee, and S. O. Hwang, "A human activity recognition method based on lightweight feature extraction combined with pruned and quantized CNN for wearable device," *IEEE Trans. Consum. Electron.*, vol. 69, no. 3, pp. 657–670, Aug. 2023.
[36] V. B. Semwal and V. Soni, "Compressed deep learning model for human activity recognition," in *Proc. IEEE Int. Students' Conf. Electr., Electron. Comput. Sci. (SCEECS)*, Feb. 2024, pp. 1–5.

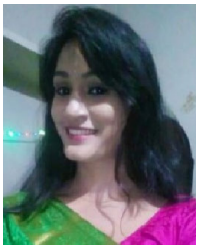

Neha Gaud (Member, IEEE) received the M.Sc. degree from the School of Computer Science, Devi Ahilya Vishwavidyalaya, Indore, India, in 2010, and the M.Phil. degree in computer science from the Institute of Computer Science, Vikram University, Ujjain, India, in 2017. She is currently pursuing the Ph.D. degree in computer science with the School of Computer Science and Information Technology, Devi Ahilya Vishwavidyalaya.

She has more than seven years of teaching experience at the Government College of Agar. She has published more than ten publications in various SCI, Scopus Journal, and refereed conferences. Her research interests include human–robot interaction, the Internet-of-Things (IoT) and wearable sensor-based health monitoring systems, and machine learning and AI.

Maya Rathore (Member, IEEE) received the master's degree in computer applications from Rajiv Gandhi Technical University, Bhopal, India, and the Ph.D. degree in computer science from Devi Ahilya Vishwavidyalaya, Indore, India.

Presently, she is working as a Professor with the CSE Department, Chameli Devi Group of Institutions, Indore. She has more than 18 years of academic experience. She has contributed 24 research publications in various national and international conferences and journals. She has co-authored a book on OOAD and published two book chapters (Springer). Her areas of research are software engineering, service-oriented computing, distributed computing, and cloud computing.

Ugrasen Suman (Senior Member, IEEE) received the master's degree in computer applications from Rani Durgawati University Jabalpur, Jabalpur, India, and the Ph.D. degree in computer science from Devi Ahilya Vishwavidyalaya, Indore, India.

He was the Dean of Engineering Sciences and a member of the Executive Council at Devi Ahilya Vishwavidyalaya. Presently, he is working as a Professor at the School of Computer Science and Information Technology. He is the Chairperson of Central BoS for designing and implementing B.Sc. (computer maintenance) syllabus as per NEP-2020 at the state level. He has more than 22 years of experience in teaching and research.

Dr. Suman was a member of BoS, DRC, CET, Proctorial Board, AntiRagging, UFM, and Flying Squad DAVV, and a member of BoS and RDC in various other universities. He has been a TPC member/an editorial member/a reviewer in various conferences and journals. He is a member of the Departmental IQAC, Planning, Assessment and Research Committee, Examination, Admission, and Anti-Ragging. He is a member of IEEE-CS, a Life Member of CSI, and a Senior Member of IACSIT and IAENG. He has been nominated as a member/a subject expert of UGC Inspections, NAAC Peer Team Visits, NBA Accreditations, AICTE Inspections, AICTE Margadarshak, AICTE Translator in SLA Project, NIELIT, Inspection Committees of DAVV, and other universities. He was the Chairperson of BoS Computer Science and IT from 2019 to 2023. He is a reviewer of IEEE TRANSACTIONS ON SOFTWARE ENGINEERING and *Journal of Software: Evolution & Process* (Wiley). He has chaired various technical sessions and delivered several expert lectures. Also, he has served as a subject expert in various selection committees in IITs, public service commissions, universities, and colleges. He has organized several workshops and the National Conference on Architecture Future IT Systems in 2008.